Construction and Building Materials 292 (2021) 123380

Contents lists available at ScienceDirect

Construction and Building Materials

journal homepage: www.elsevier.com/locate/conbuildmat

Bond coefficient, k_b, of GFRP bars

Vanessa Benzecry *, Alvaro Ruiz Emparanza, Francisco De Casoy Basalo, Antonio Nanni

Department of Civil, Architectural and Environmental Engineering, University of Miami, 1251 Memorial Dr., Coral Gables, FL 33146, United States

HIGHLIGHTS

- The current CSA/CAN 806-12 test method to determine the k_b factor has generated results with a large range of k_b values.
- The k_b results obtained with the adapted test method were compatible to the results of the CSA/CAN 806-12 test method and indicated some advantages.
- The adapted test method eliminates test errors due to manual recordings and allows to simultaneously determine the bar embedment length.
- k_b of grooved bars appeared to be slightly higher (i.e., lower bond strength) than the k_b of sand-coated helical wrap bars.

ARTICLE INFO

Article history:
Received 8 December 2020
Received in revised form 24 March 2021
Accepted 13 April 2021

Keywords:
GFRP bars
Reinforced concrete
Crack width
Testing
Design guides

ABSTRACT

Due to the increase in the number of manufacturers of GFRP bars, there is currently a variety of products in the marketplace with different physical and mechanical properties. These differences directly influence the bond coefficient, k_b, a coefficient intended to relate the behavior of GFRP to that of steel bars for the computation of crack width and deflection of reinforced concrete elements. The 2015 version of the Guide for Design and Construction of Structural Concrete Reinforced with Fiber Reinforced Polymers by ACI Committee 440 recommends a k_b value of 1.4 for bars that have not been experimentally tested. To establish a specific k_b, bars could be experimentally tested according to the 2012 edition of Canadian Standard S806-12. This test method is rather complex and has produced k_b values varying from 0.69 to 1.61 according to published literature. The study presented in this paper determined k_b according to the Canadian test method and a simpler proposed variation. This comparison is based on data derived from twenty-three beams tested to determine k_b for two types of GFRP bars (Type-A and Type-B) and a conventional steel bar (Type-S). Bar Type-A is sand-coated with a helical wrap surface treatment, while Type-B is helically grooved. The investigation yielded similar results for both test methods and indicated some advantages with the use of the proposed test method. The k_b of the Type-A presented a slightly better (lower) k_b than the Type-B.

1. Introduction

The use of Glass Fiber Reinforced Polymer (GFRP) bars in place of steel bars in reinforced concrete (RC) structures has been increasing due to their non-corrosive behavior. As a result, the number of GFRP bar manufacturers has also increased. There are currently several pultruders around the globe and each of them has its own product and manufacturing process [1]. Surface treatments of GFRP bars, for example, vary from deformed, sand-coated and grooved. Variations in constituents and manufacturing process directly influence the design and mechanical behavior of GFRP-RC elements.

The design of GFRP-RC members is generally governed by serviceability limit states, such as deflection and crack width, instead of ultimate limit states [2]. This is due to the GFRP low modulus of elasticity, when compared to that of steel bars [3]. In design guides and codes, the bond coefficient, k_b, accounts for the difference in bond behavior between GFRP and steel rebars. k_b is assumed to be 1.0 when the bond behavior of GFRP is identical to the bond of uncoated steel, higher than 1.0 if it is worse, and less than 1.0 if it is better [4]. Deflection and crack width are directly related to k_b, while k_b is dependent on the manufacturing process, mechanical properties and surface treatment of the bars. Therefore, the diversity of GFRP bars makes it difficult to develop generic, reliable and safe provisions for bond performance.

The 2015 version of the Guide for Design and Construction of Structural Concrete Reinforced with FRP Bars [4] recommends a k_b value of 1.4 for bars that have not been experimentally tested.

* Corresponding author.
E-mail addresses: v.benzecry@umiami.edu (V. Benzecry), alvaro.ruiz@miami.edu (A. Ruiz Emparanza), fdecaso@miami.edu (F. De Casoy Basalo), nanni@miami.edu (A. Nanni).

https://doi.org/10.1016/j.conbuildmat.2021.123380
0950-0618/

The recommended test to experimentally determine the k_b is described in the Canadian Standards Association CAN/CSA S806-12 [5], which correlates measured crack width to the bond coefficient, k_b, by applying Equation (1).

$$w = 2\frac{f_f}{E_f}\beta k_b\sqrt{d_{c+}^2 + \left(\frac{s}{2}\right)^2} \quad (1)$$

where

w = crack width
f_f = stress in FRP reinforcement, MPa
E_f = modulus of elasticity of FRP bar, MPa
β = ratio of distance from neutral axis to extreme tension fiber to distance from neutral axis to center of tensile reinforcement
k_b = bond coefficient
d_c = thickness of concrete cover measure from the extreme tension fiber to center of bar, mm
s = longitudinal FRP bar spacing, mm

This rather complex test method has generated results with a large range of k_b values, varying from 0.6 to 1.72 [6–15]. The large variation was confirmed by Shield et al. [16] for test data obtained following the same procedure for specimen preparation and test setup. In this case, k_b values ranged between 0.69 and 1.61.

This study presents new data obtained from experimental tests conducted on GFRP-RC beams according to both the CAN/CSA S806-12 test method and a proposed variation of this method. Accordingly, k_b of two types of GFRP bars (Type-A and Type-B) was computed. Bar Type-A is sand-coated with helical wrap surface treatment, while Type-B is made of helical grooved surface. For benchmarking, a steel bar (Type-S) was also evaluated.

2. Research significance

The experimental evaluation of k_b for different GFRP bars provides a contribution to the understanding of how bar mechanical and physical properties influence RC cracking and deflection behavior. Moreover, an improvement of a current experimental test to determine k_b can provide a simpler and more reliable method to generate data required for design.

3. Experimental program

3.1. Materials

3.1.1. Reinforcing bars

Three types of bars were used in this experimental study: two types of GFRP bars, referred to as Type-A and Type-B, and a traditional carbon steel bar Grade 420 (Type-S). Bar Type-A was sand-coated and helically wrapped while the surface enhancement of bar Type-B consisted of helical grooves. The surface treatment of the traditional carbon steel bar, Type-S, comprised standardized lugs. The bars with their different surface treatments are shown in Fig. 1.

The bars were chosen to allow for a comparison between two different surface treatments of GFRP bars. The bars used in this experiment were No. 13, with a nominal diameter of 12.7 mm and a nominal area of 129.0 mm^2 as per ASTM D7957 [17]. The latter value was used for the computation of stresses in lieu of the measured area. The No. 13 bar size was selected because is the smallest size used as longitudinal reinforcement in RC flexural elements while most suitable in terms of specimen size for laboratory equipment and space.

Prior to the design of the beam specimens, the three bar types were tested in accordance with ASTM standards to obtain their tensile strength and elastic modulus. The tensile test for the GFRP bars was performed in accordance with ASTM 7205 [18], while the tensile test for the steel bars were performed following ASTM A615/615-M-16 [19]. The area of the bars used to calculate strength was the nominal value per ASTM 7957 [17]. A minimum of five test repetitions were performed per bar type. The results of the tensile tests are shown in Table 1.

Fig. 1. Bar types. From the left: GFRP Type-A, GFRP Type-B and steel Type-S.

It can be observed from the test results that GFRP bars have a modulus of elasticity about four times lower than that of steel bars. Their tensile strength, however, was about 70% to 125% higher than the yield strength of the steel bars. It is important to note that the rupture strength of steel bars, f_u, was about 53% higher than the yield strength, f_y, but still lower than the ultimate strength of the GFRP bars, as seen in Fig. 2.

3.1.2. Concrete

The concrete used for the experiments was a Florida Department of Transportation (FDOT) approved Class II 4500 Bridge Deck mix design as shown in Table 2. This is a normal weight concrete with a theoretical 28-day compressive strength of 31 MPa. The concrete slump was obtained in accordance with ASTM C143/C143M [20] and recorded to be about 900 mm. All beams were cast with the same concrete batch and cylinders of dimensions 100 × 200 mm were collected during casting for compressive strength determination. Cylinders were tested at various ages in accordance with ASTM C39 [21] to obtain the compressive strength progression with time and finally at 28-day (see Fig. 3). The five-specimen 28-day strength average was 42.6 MPa with a standard deviation of 1.1 MPa (coefficient of variation of 2.6%).

3.2. Beam design

The beams were designed in accordance with ACI 440.1R-15 [4] with the controlling limit state of FRP rupture or tension failure (i.e., bar failure to occur prior to concrete crushing). To ensure tension failure, the reinforcement ratio must be lower than the balanced reinforcement ratio (ρ_b). The minimum FRP reinforcement requirements were also checked to prevent sudden failure upon concrete cracking. The reinforcement ratio for each beam and their flexural capacity are shown in Table 3.

For this study, two different beam designs were used, one following CAN/CSA 806-12 approved test method to determine k_b, and the other using a variation of this method. Both designs used top bars for constructability purposes only; thus, the top bars were interrupted over the constant moment region (four-point approved test) and over the central 100 mm (three-point adapted test). It is

Table 1
Bars mechanical properties.

Rebar Type	Surface Enhancement	Ultimate Tensile Properties			
		Load (kN)	Strength (MPa)*	Strain (%)	E-modulus (GPa)
Type-A	sand-coated and helical wrap	103.8 ± 6.8	804.1 ± 38.9	1.61 ± 0.06	50.15 ± 2.7
Type-B	helical grooves	134.3 ± 6.6	1040.6 ± 51.0	1.78 ± 0.07	58.52 ± 2.21
Type-S	lugs	90.6 ± 3.5	702.3 ± 27.4	6.1 ± 0.3	211.41 ± 6.1

* Note: Based on nominal area

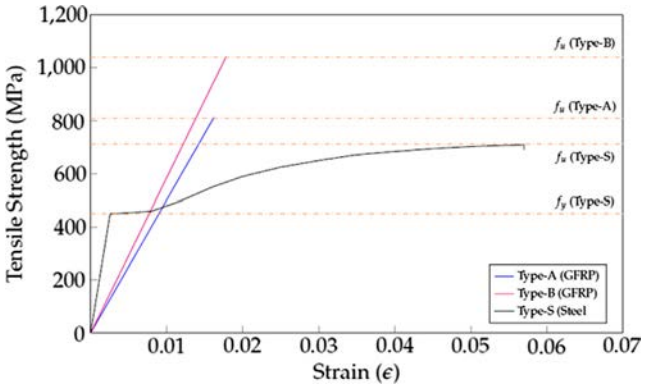

Fig. 2. Stress–strain curves for the three types of reinforcement.

Table 2
Concrete mix design.

Concrete mix design		
Cement Type II	83.5	kg/m^3
SlagSlag	126.9	kg/m^3
#57 Stone	544.1	kg/m^3
Silica Sand	461.2	kg/m^3
Water	94.1	kg/m^3
Air entraining (AE 90)	67.8	g/m^3
Type-D Admixture (retarder and reducer)	271.4	g/m^3

noted that if top bars were to be continuous, in order to prevent them from acting as tension reinforcement, they should always be placed above the cracked neutral axis.

The k_b test proposed by CAN/CSA 806-12 [5] consists of a four-point flexural test. In total, eight beams were cast but only seven were adequate for testing. Three beams were reinforced with Type-A bars, two with Type-B bars, and the remaining two with Type-S bars. For each specimen, two No. 13 bars were placed at the bottom of the beam as seen in Fig. 4. To prevent the beams from failing in shear, No. 10 steel stirrups at 150 mm on-center were used along the beam, except on the center portion of the specimen, where shear is zero. To hold the stirrups in place, two No. 13 bars were used as top reinforcement. Top bars were not included on the center portion (L/3) of the beam, where the moment is constant. The final design of the beams consisted of 3350 mm in length with a 3050 mm span and a cross section size of 200 mm × 356 mm. The details of the specimen are shown in Fig. 4.

For the sixteen beams designed in accordance with the adapted test procedure, six were reinforced with Type-A bars, six with Type-B bars and four with Type-S bars. This method uses a three-point flexural test, which is more practical for smaller beams (suitable for laboratories) and its combination for shear and moment may be a better representation of field situations.

The bottom (tension) reinforcement comprised only one bar; however, spliced as shown in Fig. 5. The bars were No. 13 bars, with one of the bars extending beyond the mid-span of the beam for a length corresponding to the embedment length. The other two bars extended 50 mm passed the mid-span of the beam, leaving the midspan reinforced with a single rebar as seen in Fig. 6. The embedment length was initially calculated as per ACI 440.1R development length. It was found to be 91 times the rebar diameter (d_b) (1155 mm) for bar Type-A; 125 d_b (1595 mm) for bar Type-B; 36 d_b (460 mm) for steel bars based on yield stress and 55 d_b (700 mm) based on steel rupture. However, as a result of preliminary testing, these values were found to be very conservative. It was observed that the GFRP bars required a minimum embedment length of 40 d_b to ensure the failure of the bars while the steel bars required 30 d_b. Consequently, with the additional objective to

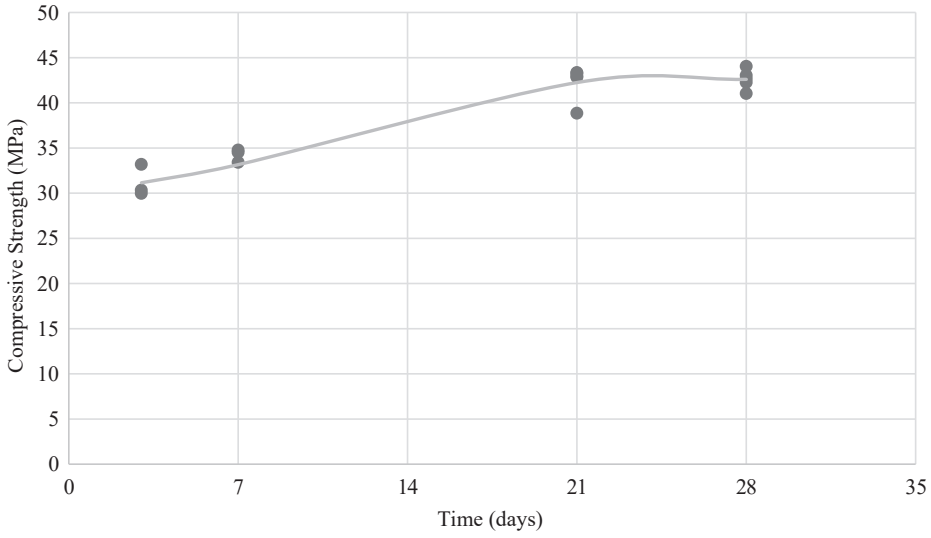

Fig. 3. Concrete compressive strength test results.

Table 3
Beams design parameters per reinforcement type.

Bar Type	Test Method	Reinforcement ratio ρ_f	Balanced Reinforcement Ratio (ρ_b)	ρ_f/ρ_b	Location of cracked N.A. (mm)	Theoretical Flexural Capacity	
						P_n (kN)	M_n (kN-m)
Type-A	Approved	0.00421	0.00667	0.6306	56	81.8	43.4
	Adapted	0.00276	0.00526	0.5247	31	79.9	30.4
Type-B	Approved	0.00421	0.00562	0.7488	60	104.1	55.6
	Adapted	0.00276	0.00372	0.7419	33	104.0	39.5
Type-S	Approved	0.00421	0.0311	0.1403	89	59.6	31.2
	Adapted	0.00276	0.03374	0.0818	55	69.3	26.3

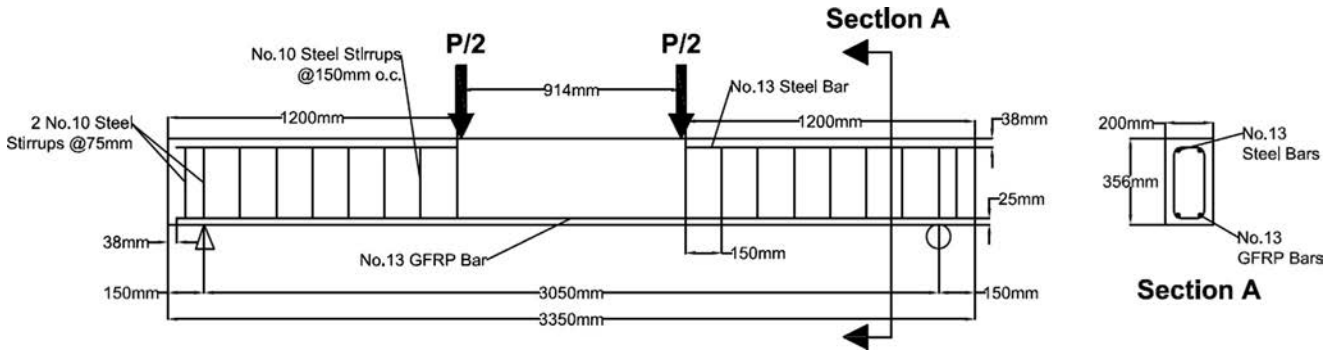

Fig. 4. Reinforcement plan – beams using approved test method.

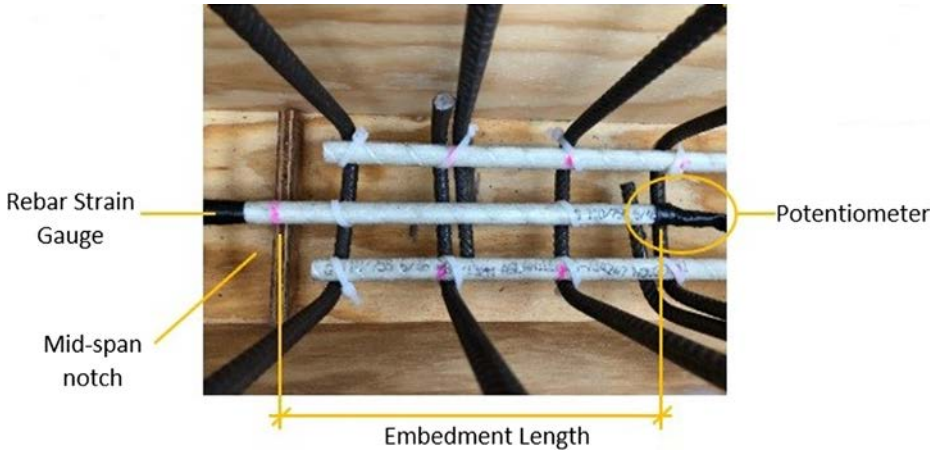

Fig. 5. Adapted test beam – bar splice detail.

investigate the required embedment length for a full stress transfer between a GFRP bar and concrete, the chosen embedment lengths for beams reinforced with GFRP bars were 50, 60 and 70 d_b, and for the beams reinforced with steel bars were 30, 40 and 70 d_b. The 70d_b was chosen to have both reinforcing systems with the same embedment length.

This configuration enables both the investigation of the bar embedment length and k_b at the same time. For this study, because the objective was to evaluate the k_b only, the different splice lengths selected were ensured to exceed the minimum embedment length requirement to perform as a continuous bar, and therefore, do not influence the k_b results. The minimum embedment lengths, however, may vary for GFRP bars from different manufacturers. Therefore, his test method allows the use of different lengths to determine the minimum embedment for each bar type.

To prevent the beam from failing in shear, No. 10 stirrups at 75 mm on center were used and No. 10 top bars were used to secure the stirrups in place. The center portion of the beam (100 mm), where the moment is at maximum, was left free of top reinforcement. Another novelty of this test procedure was that the beams were notched at midspan to induce a localized crack and ease crack monitoring, as this is one of the main difficulties with the CAN/CSA-806 test method. The final design of the beams consisted of specimens of 1830 mm in length with a span of 1520 mm and a cross of 360 mm × 150 mm. The details of the specimen are shown in Fig. 6.

4. Instrumentation

The beams were instrumented to monitor applied load, crack width, deflection and strain throughout the test. To record the

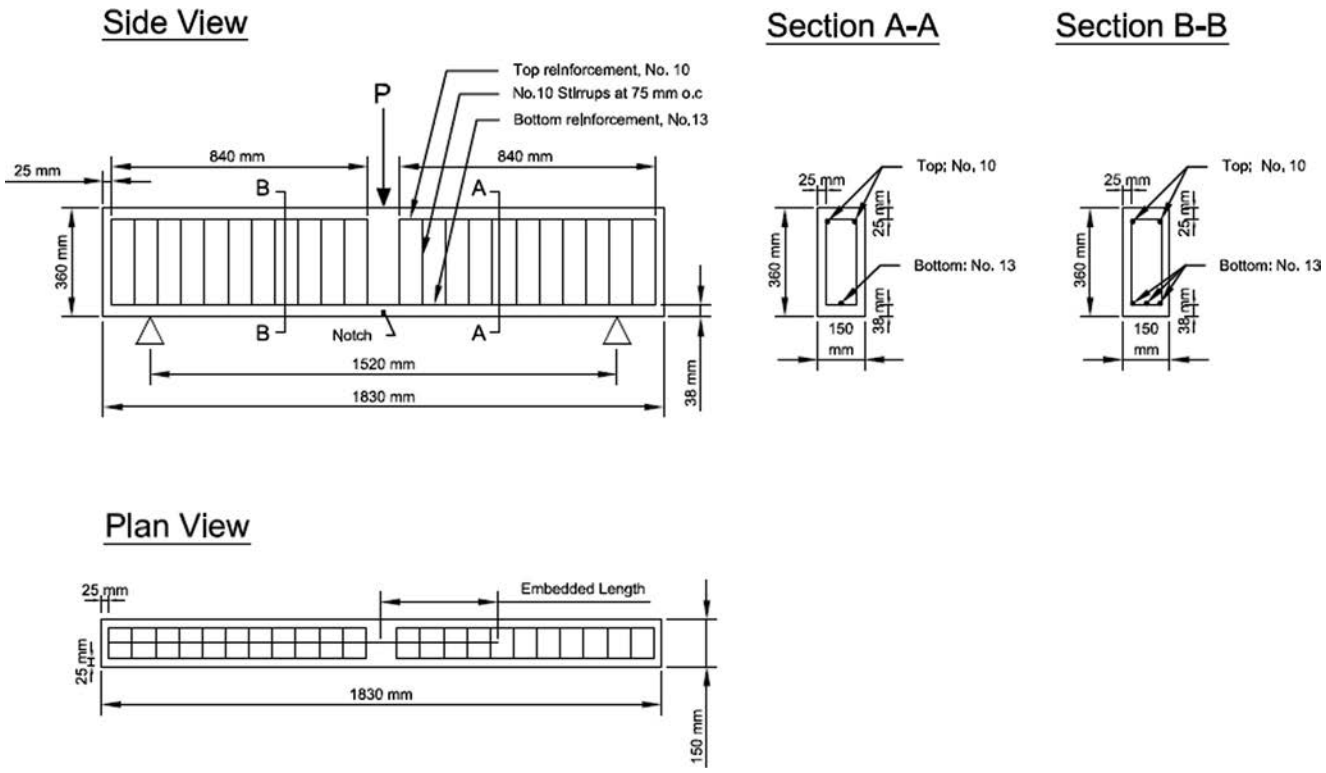

Fig. 6. Reinforcement plan – beams using adapted test method.

strain in the reinforcement, two 6-mm strain gauges were placed on the midspan of the bottom reinforcement (prior to casting the beams), one on each rebar for the approved method and two on the main tensile bar for the adapted method. To record the compressive strain of the concrete, two 50-mm strain gauges were installed on the top side of each beam (once the concrete had cured and the beams were ready to be tested). To record crack widths, each beam used two Linear Variable Differential Transducers (LVDTs). The LVDTs used in the approved test method were place on the beam at the moment of appearance and location of the first and second crack, while the LVDTs used in the adapted test method were placed on both lateral faces of the beam at the location of the notch prior to the start of the test since the notch induced the crack at a known location. In both tests, the two LVDTs used to measure crack width were placed horizontally at the level of reinforcement. Additional LVDTs were also placed at mid-span to record mid-span deflection.

In addition, the adapted test procedure included a potentiometer at the location of the spliced bars to monitor the slippage of the rebar. The slippage of the bar is monitored to verify and determine the minimum embedment length of the GFRP bar. The potentiometer had a 40.4 mm long shaft that enabled the measurement of bar displacement up to 6.35 mm as it can freely move through the main body of the potentiometer.

The beams tested in accordance with CAN/CSA S806-12 were tested using the Baldwin test frame under four-point bending (Fig. 7). The load was applied by a 267 kN hydraulic jack. A load cell was placed in between the hydraulic jack and the spreader beam to monitor the applied load. Finally, the strain of the reinforcement was recorded using two strain gauges. All the instrumentation was connected to a centralized data logger for a synchronized data collection. The data acquisition frequency was set at10 Hz.

For the beams investigated using the adapted test procedure, a universal MTS test frame was used for a three-point flexural test (Fig. 8). The test set up consisted of a simple supported beam with a midspan point load, which was applied by a 240 kN hydraulic jack. Three LVDTs were placed at the center of the specimen, one recording the mid-span displacement and two recording the crack widths induced by the concrete notch at midspan. Finally, the strain of the reinforcement was recorded using two strain gauges. All the instrumentation was connected to a centralized data logger for a synchronized data collection. The data acquisition frequency was set at 10 Hz.

5. Test set-up and procedure

A total of twenty-three full-scale simply supported beams were designed, constructed and tested.

5.1. CAN/CSA 806-12 method

The load was applied quasi-statically to the specimen at a displacement-controlled rate of 1.9 mm/min until the appearance of the first crack. Once the first crack was observed, the load was stopped, and the crack was mapped and measured with a hand-held optical microscope. An LVDT was placed at the location of the first crack to measure and monitor the crack width until the end of the test. The load was resumed until a second crack was observed. The second crack was again mapped, and a second LVDT was placed at that location to monitor the crack width until the end of the test. The load was resumed until the specimen failed.

5.2. Adapted method

The loading was conducted in two phases. In the first phase, the load was applied in load control mode at a rate of 22 N/s for a total of eight cycles. Each cycle had load steps at: 50%, 67%, 83% and 100% of a load magnitude defined as 85% of the ultimate load capacity as per ACI 440-1R-15 [4]. At each load step, the load was held constant for two minutes. In the second phase, the beam

Fig. 7. CAN/CSA 806-12 test setup.

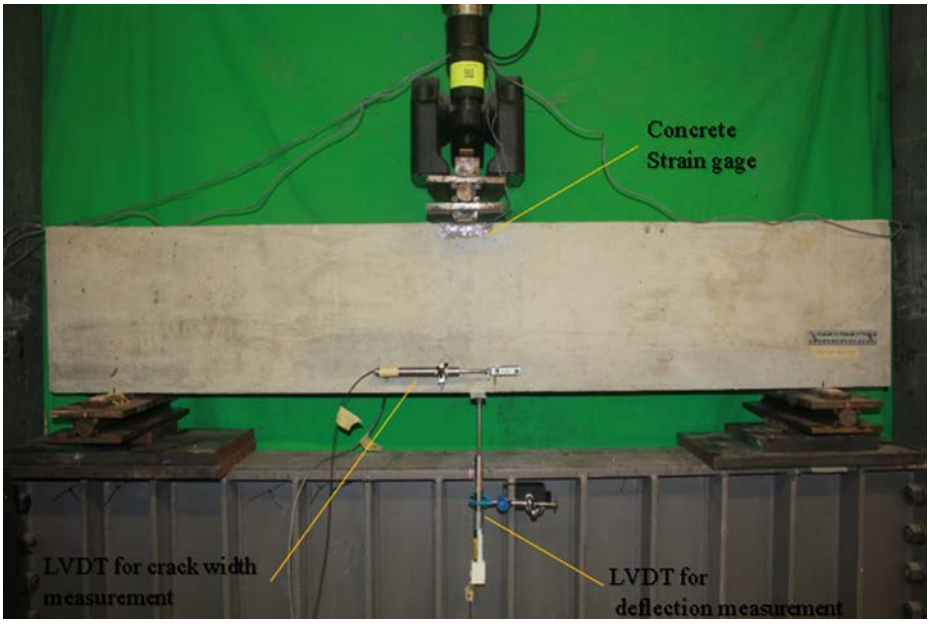

Fig. 8. Adapted test method setup.

was loaded in displacement control at a rate of 0.317 mm/s until failure. The change between load control and displacement control was chosen to avoid a catastrophic collapse and to observe the behavior of the beam after the peak load was reached. This procedure mirrors the recommendations of ACI 437-12 [22].

6. Observations

As part of the objective to improve the test method and the accuracy of results, this section points out to issues observed during the research. The first concern with the approved test method [5] is related to the measurement of the crack width, which is the basis for obtaining the k_b. Following CSA guidelines, k_b is calculated from the measured crack width of the first and second flexural cracks observed during the four-point flexural test. However, more than two flexural cracks may form nearly at the same time during the test. This generates uncertainties in determining the time initiation and location of the first and second crack, resulting in variability in the size of the crack width as the load increases. Furthermore, this method relies on manual readings and device installation as the test is in progress, thus increasing the chance of errors.

Another inconsistency with the approved test method relates to the crack width to be used for k_b calculation. In fact, the test guidelines do not specify what crack width to use in the formula: should it be the first crack, the second crack width or the sum of the two? The only specification on the guidelines is that the crack width, *w*,

should not exceed 0.7 mm. In addition, the guideline suggests that the k_b should be the average of the values obtained using different crack widths: should k_b be calculated based on repetitions or with only a single crack width measurement? Both methods to calculate k_b, by averaging values and by selecting one specific crack width, can lead to inconsistent k_b values. Shield et al. [16] observed that small crack widths can lead to small values of k_b, while larger crack widths can lead to very conservative k_b values.

Looking beyond the outlined CSA procedure, there is no standard approach to calculate k_b. Two methods have been proposed by researchers, one using the FRP stress-level [23–25] and the other using the slope of the FRP strain vs. crack width [6,26]. The stress-level approach derives the k_b by using the observed experimental crack width at a specified FRP stress-level. The slope approach utilizes the slope of the best fitting linear curve of FRP strain vs. crack width, which gives an average (smeared) value. Both approaches have their weaknesses. The stress-level approach can provide inconsistency due to the variability of FRP tensile strength and, therefore, the difficulty in selecting a specific stress level, while the slope approach can produce a low k_b due to the wide range of crack widths.

7. Results and discussion

In terms of specimen parameters, the main change implemented in the adapted test method to determine the k_b was the presence of the notch at mid-span to induce the crack formation at a selected location versus multiple locations that may be difficult to identify. Additionally, a three-point load configuration decreases the likelihood of additional cracks. The crack width for the adapted test was measured by two LVDTs, one on each side of the beam and during the entire duration of the test. For the approved method, the crack width used for the evaluation of the k_b included the values recorded by the two LVDTs, one for each crack (first and second) plus an initial crack width developed prior to the placement of the LVDT.

The approach taken to calculate k_b for both test methods was based on the maximum crack width. The maximum crack width allowed to be used in Eq. (1) according to CSA/CAN 806-12 is 0.7 mm. This value is also the maximum crack width considered acceptable for aesthetics reasons in accordance with ACI-4401R-15 [4]. Consequently, k_b for both test methods was calculated at a crack width equal to 0.7 mm for the GFRP-RC beams. Similarly, for the steel-RC beams, k_b was calculated at a crack width of 0.18 mm. This value is the limiting crack width specified by the Control of Cracking in Concrete Structures ACI 224R-01 [27] for structures exposed to deicing salts. Although, ACI 224-R-01 [27] specifies different crack width limits per structure type, this limit was chosen as it is the threshold for structures subjected to aggressive environments, which is the focus of FRP reinforcement application.

The k_b for both cases was calculated by averaging the values (of load, moment and strain) obtained for both cracks when the crack width was equal to 0.7 mm (for GFRP bars, and 0.18 mm for steel bars). The GFRP strains used in the calculation of k_b were the analytical values calculated assuming a cracked elastic section. The summary of the k_b results including load, moment and strain, are shown in Table 4.

Table 4
Experimental beams results.

Rebar Type	Beam ID	Test Method	Load kN	Moment kN-m	Strain Theo με	Bond Factor, k_b	kb /k_b steel
Type-A	50-001	Adapted	18.74	7.12	3584	1.01	1.16
	60-001	Adapted	15.93	6.06	3273	1.12	1.29
	60-002	Adapted	16.04	6.09	3067	1.19	1.37
	70-001	Adapted	19.2	7.3	3673	0.99	1.14
	70-002	Adapted	21.11	8.02	4038	0.92	1.06
	70-003	Adapted	22.55	8.57	4312	0.89	1.02
					average	1.02	1.17
					std. dev.	0.12	0.13
	A-002	Approved	47.08	25.19	6196	0.91	1.05
	A-005	Approved	37.22	19.92	4899	1.16	1.33
	A-008	Approved	40.17	21.49	5287	1.08	1.24
					average	1.05	1.21
					std. dev.	0.13	0.15
Type-B	50-001	Adapted	16.50	6.37	2721	1.33	1.53
	60-001	Adapted	23.80	9.05	3926	1.08	1.24
	60-002	Adapted	15.57	5.92	2566	1.41	1.62
	70-001	Adapted	21.57	8.19	3555	1.02	1.17
	70-002	Adapted	22.56	8.57	3718	0.97	1.11
	70-003	Adapted	24.44	9.29	4029	0.9	1.03
					average	1.12	1.29
					std. dev.	0.21	0.24
	A-001	Approved	48.25	25.81	5642	1.02	1.17
	A-004	Approved	35.98	19.29	4207	1.34	1.54
					average	1.18	1.36
					std. dev.	0.16	0.18
Type-S	30-001	Adapted	28.06	10.67	1270	0.81	0.93
	30-002	Adapted	26.96	10.24	1271	0.73	0.84
	40-001	Adapted	22.97	8.73	1037	0.9	1.03
	40-002	Adapted	20.85	7.92	999	0.93	1.07
					average	0.84	0.97
					std. dev.	0.09	0.10
	A-003	Approved	49.17	26.31	1614	0.88	1.01
	A-007	Approved	44.14	23.62	1491	0.97	1.11
					average	0.93	1.06
					std. dev.	0.045	0.05

* Note: overall average k_b of bars Type-S equal to 0.87.

The most important observation is in that both tests yielded similar k_b results. This is an indication that the crack-width approach chosen to calculate k_b may reduce inconsistencies. The overall average k_b for Type-A bars was 1.03 with a coefficient of variation (COV) of 11%, while the overall average k_b for Type-B was 1.13 with a COV of 17%. The steel bars presented a k_b average of 0.87 with a COV of 10%.

If the experimental value of k_b for steel (overall average = 0.87) as determined in this study is used as reference, then the average k_b of Type-A bars would become 1.18, and the average k_b of Type-B bars would become 1.31. The k_b of Type-B bars, with helical grooves, is higher than the k_b of Type-A bars with sand-coated surface. This was also observed in other studies [16,28,29,25], although the difference between the k_b values in this study is smaller.

8. Conclusions

Twenty-three beams were tested according to both the CAN/CSA 806-12 test method and a proposed variation of this method called "adapted test method". k_b was investigated for two types of GFRP bars, Type-A made of sand-coated with helical wrap surface treatment and Type-B made of helical grooved surface treatment. A steel bar, Type-S, was included for benchmarking. From the observations and results of the experimental tests, the following conclusions can be made:

- The current CSA/CAN 806-12 test method leaves room for error and dissimilarity among experiments from different studies. The main cause of disparity identified during this study was the location of the crack and the crack width used in the calculation of k_b.
- The proposed approach to use the maximum crack width (w = 0.7 mm for GFRP bars) was found to provide consistent k_b results among experiments and, therefore, is the recommended approach
- The results of the adapted test were compatible to the results of the CSA/CAN 806-12 test method and indicated some advantages. The notched concrete used in the adapted test method facilitates the measurement and monitoring of the crack width and eliminates test errors due to manual recordings. The use of spliced bars as the tension reinforcement allows this test to be simultaneously used to determine the required embedment length for the GFRP bars.
- k_b of grooved bars appeared to be slightly higher than the k_b of sand-coated helical wrap bars.
- This study contributes to literature's experimental data on k_b, and helps identify areas that can be improved to promote the safe application of FRP and assist in the development of design codes.

CRediT authorship contribution statement

Vanessa Benzecry: Conceptualization, Methodology, Validation, Investigation, Writing - original draft. **Alvaro Ruiz Emparanza:** Conceptualization, Methodology, Validation, Investigation, Writing - review & editing. **Francisco De Casoy Basalo:** Conceptualization, Resources, Writing - review & editing, Supervision. **Antonio Nanni:** Conceptualization, Funding acquisition, Writing - review & editing, Supervision.

Declaration of Competing Interest

The authors declare that they have no known competing financial interests or personal relationships that could have appeared to influence the work reported in this paper.

Acknowledgments

The authors gratefully acknowledge the partial financial support from the NSF Center for Integration of Composites into Infrastructure (CICI) under grant #1916342. In-kind support was graciously provided by the concrete supplier, Supermix, and two GFRP manufacturers, Pultron Composites and Owens Corning.

References

[1] A.R. Emparanza, R. Kampmann, Y. De Caso, F. Basalo, State-of-the-practice of global manufacturing of FRP rebar and specifications, Special Publication 327 (2018) 45–51.
[2] C. Barris, L. Torres, A. Turon, M. Baena, A. Catalan, An experimental study of the flexural behaviour of GFRP RC beams and comparison with prediction models, Compos. Struct. 91 (3) (2009) 286–295.
[3] S.R. Mousavi, M.R. Esfahani, Effective moment of inertia prediction of FRP-reinforced concrete beams based on experimental results, J. Compos. Constr. 16 (5) (2012) 490–498.
[4] ACI Committee 440. (2015). Guide for the Design and Construction of Structural Concrete Reinforced with Fiber-Reinforced Polymer (FRP) Bars (ACI 440. 1R-15). Farmington Hills, Michigan: American Concrete Institute.
[5] Canadian Standards Association, CAN/CSA S806-12 Design and construction of building structures with fibre-reinforced polymers, (2012).
[6] C.E. Bakis, C.E. Ospina, T.E. Bradberry, B. Benmokrane, S.P. Gross, J. Newhook, G. Thiagarajan, December). Evaluation of crack widths in concrete flexural members reinforced with FRP bars, in: Third International Conference on FRP Composites in Civil Engineering, 2006, pp. 307–310.
[7] E.F. El-Salakawy, B. Benmokrane, Serviceability of concrete bridge deck slabs reinforced with FRP composite bars, ACI Struct. J. 101 (5) (2004) 727–736.
[8] R.G. Giernacky, Durability of E-glass FRP reinforced concrete beams B.S. thesis, Dept. of Engineering Science and Mechanics, Penn State Univ., 2002.
[9] C. Kassem, Cracking and load-deflection behaviour of one-way concrete elements reinforced with FRP bars under flexure [In French.] Ph.D. thesis, Dept. of Civil Engineering, Université de Sherbrooke, 2004.
[10] R. Masmoudi, M. Theriault, B. Benmokrane, Flexural behavior of concrete beams reinforced with deformed fiber reinforced plastic reinforcing rods, Struct. J. 95 (6) (1998) 665–676.
[11] J.P. Newhook, The use of fibre reinforced concrete to reduce crack widths in GFRP reinforced concrete beams, in: Proc. 3rd Intl. Conf. Advanced Composite Materials in Bridges and Structures, 2000, pp. 145–152.
[12] P.M. Theisz, Properties of high performance concrete beams reinforced with carbon fiber reinforced polymer bars Doctoral dissertation, Villanova University, 2004.
[13] M. Theriault, B. Benmokrane, Effects of FRP reinforcement ratio and concrete strength on flexural behavior of concrete beams, J. Compos. Constr. 2 (1) (1998) 7–16.
[14] G. Thiagarajan, Experimental and analytical behavior of carbon fiber-based rods as flexural reinforcement, J. Compos. Constr. 7 (1) (2003) 64–72.
[15] D. Trejo, F. Aguiniga, R.L. Yuan, R.W. James, P.B. Keating, (2005). Characterization of design parameters for fiber reinforced polymer composite reinforced concrete systems (No. FHWA/TX-5/9-1520-3).
[16] C. Shield, V. Brown, C.E. Bakis, S. Gross, A recalibration of the crack width bond-dependent coefficient for GFRP-reinforced concrete, J. Compos. Constr. 23 (4) (2019) 04019020.
[17] ASTM D7957/D7957M-17. Standard Specification for Solid Round Glass Fiber Reinforced Polymer Bars for Concrete Reinforcement, ASTM International, West Conshohocken, PA, (2017).
[18] ASTM D7205/D7205M-06, Standard Test Method for Tensile Properties of Fiber Reinforced Polymer Matrix Composite Bars, ASTM International, West Conshohocken, PA (2016).
[19] ASTM A615/A615M-16, Standard Specification for Deformed and Plain Carbon-Steel Bars for Concrete Reinforcement, ASTM International, West Conshohocken, PA. (2016).
[20] ASTM C143/C143M. Standard Test Method for Slump of Hydraulic-Cement Concrete, ASTM International, West Conshohocken, PA, (2015).
[21] ASTM C39/C39M-16, Standard Test Method for Compressive Strength of Cylindrical Concrete Specimens, ASTM International, West Conshohocken, PA (2016).
[22] ACI Committee, 437-12: Code Requirements for Load Testing of Existing Concrete Structures and Commentary (an ACI Provisional Standard). Farmington Hills, Michigan: American Concrete Institute. (2012).
[23] A. El-Nemr, E.A. Ahmed, C. Barris, B. Benmokrane, Bond-dependent coefficient of glass-and carbon-FRP bars in normal-and high-strength concretes, Constr. Build. Mater. 113 (2016) 77–89.
[24] F. Elgabbas, E.A. Ahmed, B. Benmokrane, Flexural behavior of concrete beams reinforced with ribbed basalt-FRP bars under static loads, J. Compos. Constr. 21 (3) (2017) 04016098.

[25] C. Kassem, A.S. Farghaly, B. Benmokrane, Evaluation of flexural behavior and serviceability performance of concrete beams reinforced with FRP bars, J. Compos. Constr. 15 (5) (2011) 682–695.
[26] W.K. Lee, D.C. Jansen, K.B. Berlin, I.E. Cohen, Flexural cracks in fiber-reinforced concrete beams with fiber-reinforced polymer reinforcing bars, Am. Concr. Inst. Struct. J. 107 (3) (2010) 321.
[27] ACI Committee 224, Control of Cracking of Concrete Structures (ACI 224R-01). Farmington Hills, Michigan: American Concrete Institute (2008).
[28] A. El-Nemr, E.A. Ahmed, A. El-Safty, B. Benmokrane, Evaluation of the flexural strength and serviceability of concrete beams reinforced with different types of GFRP bars, Eng. Struct. 173 (2018) 606–619.
[29] A. El-Nemr, E.A. Ahmed, B. Benmokrane, Flexural behavior and serviceability of normal-and high-strength concrete beams reinforced with glass fiber-reinforced polymer bars, ACI Struct. J. 110 (6) (2013) 1077.